RSC Mechanochemistry

ROYAL SOCIETY OF CHEMISTRY

PAPER

View Article Online
View Journal

Cite this: DOI: 10.1039/d5mr00129c

Ab initio force prediction for single molecule force spectroscopy made simple

Pooja Bhat, †[ab] Wafa Maftuhin †[ac] and Michael Walter †*[abd]

Received 14th October 2025
Accepted 3rd January 2026

DOI: 10.1039/d5mr00129c

rsc.li/RSCMechanochem

Bond rupture under the action of external forces is induced by temperature fluctuations. We show that measured forces from single molecule force spectroscopy experiments can be predicted from two quantities describing the bond that are the barrier to break the bond in absence of force as well as the maximal force the bond can withstand. The former can be obtained by a force-free transition state calculation and the latter is determined by a simple constrained geometry simulates forces (COGEF) calculation. Considering experimental temperature and force loading rate allows the prediction of measured bond rupture forces from a closed expression with very good accuracy.

Introduction

Mechanochemistry is the change or modification of chemical bonds through the action of mechanical forces. It allows for modification of materials *via* the application of external forces which are usually acting in the form of external stress. External forces offer the possibility to enable reactions that are improbable or not possible by other means, such as thermal or optical activation alone.[1,2] Examples are the force induced change of ceiling temperature in a polymer[3] or enabling reactions not thermally allowed by Woodward–Hoffmann rules.[4–6]

Mechanochemistry acts on the molecular level, where bonds are broken or reformed, but mechanical forces are often applied to materials in rather unspecific methods like ball milling or ultra-sonification, where the force acting on specific bonds within the material is hard to control. Also the modification of molecular bonds by stretching of polymeric material[7] and the application of rheological methods[8] is complex due to the not well understood force distribution in complex materials, despite recent advances in this direction.[9–11]

The cleanest experimental observation of mechanochemical effects is given by measuring molecular forces in single molecule force spectroscopy (SMFS) experiments.[4,6,12–17] Here, single polymer chains are stretched and force plateaus are observed when multiple bonds in monomers are broken.[6] It is well understood that these plateaus reflect properties of the monomers experiencing the bond break.[18] The force at bond break can also be determined from a sudden drop in the force extension curve.[19–21] The numerical determination of force dependent barriers has been successfully employed by several groups[22–26] and it was shown that experimental force–extension curves can be reproduced based on properties determined from *ab initio* calculations.[18,27] Interestingly, often the properties of the monomer are sufficient to characterize the measured rupture forces.[18]

The most straightforward computational strategy to describe the effect of forces within calculations is probably the constrained geometry simulates forces (COGEF) method developed by Beyer.[28,29] It is therefore applied in many mechanochemical investigations.[30–32] The prediction of measured forces directly from COGEF has not been successful,[32] as the forces obtained are up to an order of magnitude larger than the measured ones.[33] The underlying reason is the lack of consideration of temperature[8,12,34,35] as it is the temperature fluctuations that allow to overcome the barriers for bond breaking.[36] Due to the stochastic nature of these fluctuations, only the most probable forces for bond rupture can be given. Recent investigations[37,38] use empirical correlations between the force-free bond strength and force *vs.* length correlations to fit a linear model to existing experimental data in order to obtain some predictive power.

The determination of most probable forces has a long history and several expressions were derived mainly to analyse bond rupture or friction experiments.[39–44] Expressions for most probable forces were given by Garg[39] in a very general form. These were then used by Hummer, Dudko and co-workers.[41] Rebinding effects occurring at low applied forces and slow pulling speed were considered also.[43,45]

Here we address the question of how the most probable force measured in experiment can be predicted from *ab initio* calculations without the need to fit to experimental data. We show that the experimentally measured force is mainly determined by two quantities describing the bond: its dissociation energy and the maximal force the bond can withstand. These

[a]FIT Freiburg Centre for Interactive Materials and Bioinspired Technologies, University of Freiburg, Freiburg, Germany. E-mail: Michael.Walter@fmf.uni-freiburg.de
[b]Cluster of Excellence LivMatS @ FIT, Freiburg, Germany
[c]Universitas Negeri Surabaya, Surabaya, Indonesia
[d]Fraunhofer IWM, MikroTribologie Centrum μTC, Freiburg, Germany
† These authors contributed equally.

two quantities can be obtained from *ab initio* calculations of the monomer.

The manuscript is organized as follows. We first formulate the theory and assumptions underlying our description of the bond rupture processes, where we detail the properties of the force dependent probability functions determining the most probable force. The effects of the speed of force increase (the loading rate) and the temperature are discussed. We then apply our description to published SMFS data. The paper ends with conclusions.

Results and discussion

Theory

We first consider an isolated bond of length d to develop our description. We treat bond breaking in a probabilistic picture in the spirit of Kauzman, Eyring, Evans and Ritchie[46,47] where the bond potential $U(d)$ is modified by the external force as illustrated in Fig. 1, where d denotes the bond length. The force F is aligned to the direction of the bond (the bond can rotate freely).[48] Subtracting the work performed on the molecule by the force F leads to the enthalpy[36]

$$H(F;d) = U(d) - Fd \tag{1}$$

from which the force dependent barrier $\Delta H^{\ddagger}(F)$ (*i.e.* the force dependent energy difference between the bound initial state and the transition state) can be obtained. The restriction to a given external force is a change in variables, such that the equilibrium bond length d_0 is not a free variable anymore, but gets a function of F, *i.e.* $d_0 = d_0(F)$. This is reflected by the slight shift of the minimum for finite F as compared to $F = 0$ in the potentials shown in Fig. 1. The force-free energy needed to open the bond $\Delta U^{\ddagger}$ transfers to a barrier $\Delta H^{\ddagger}(F)$ for finite force.

Apart from the bond-strength $\Delta U^{\ddagger}$ often considered, there is another fundamental property of the bond, $F_{\max}$. This is the maximal force it can withstand, *i.e.* the maximal spatial derivative of $U(d)$. It turns out, that the force dependence of the barrier $\Delta H^{\ddagger}(F)$ for many potentials can be expressed to good approximation in the form[35,36]

$$\Delta H^{\ddagger}(f) = \Delta U^{\ddagger}(1 - f)^2, \tag{2}$$

where $f = F/F_{\max}$. This is the barrier that results from a cusp-like cut quadratic potential considered by many authors.[40–43] Linearizing eqn (2) to the small force limit leads to the famous Bell barrier[29,49]

$$\Delta H^{\ddagger}(F) = \Delta U^{\ddagger} - Fx^{\ddagger} \tag{3}$$

where we identify the Bell length as $x^{\ddagger} = 2\Delta U^{\ddagger}/F_{\max}$. This length constant is often interpreted as the distance between initial and transition state,[50] despite that the latter depends on the force F itself.[36] Here, $x^{\ddagger}$ is purely defined by the two constants of the potential $\Delta U^{\ddagger}$ and $F_{\max}$.[20,36]

We now use the approximate form of the barrier in eqn (2) to derive the most probable force for bond rupture measured in the experiment under the assumption of a constant loading rate (rate of force increase). In order to illustrate the steps taken, we consider a simple linear $AuAg_2$ toy molecule (depicted in Fig. 2) described by its potential energy obtained from effective medium theory as implemented in the atomic simulation environment (ASE).[51] The potential in Fig. 1 is that of this model molecule where d is the length of the weaker Ag–Ag bond and the force F is considered to be applied to the two silver atoms directly.

It is practically impossible to apply an external force directly on two bound atoms in reality. There are always other atoms and bonds mediating the external force to the bond that ruptures. We mimic this fact in a very simplistic picture by the additional Au atom representing the environment through which the force is transferred. When a force acts on the outer atoms, the atoms respond by arranging into a new minimum energy configuration. This situation can be simulated by displacing the outer atoms using the COGEF strategy and relaxing all other degrees of freedom. This in turn gives the corresponding force needed to stabilize the given outer length. Increasing the outer distance eventually leads to rupture of the Ag–Ag bond for $\Delta U^{\ddagger} = 1.80$ eV in our example. The maximal outer force appearing in this process is $F_{\max} = 2.38$ nN. These

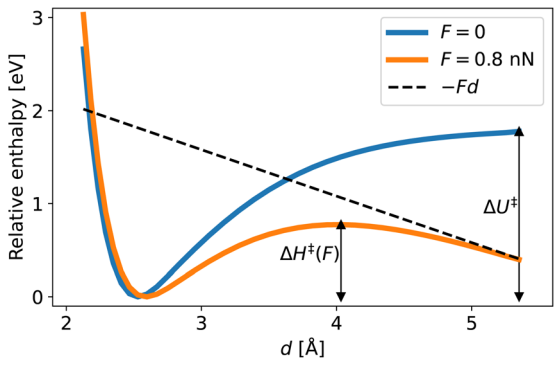

Fig. 1 Force dependent potentials according to eqn (1) of the $AuAg_2$ model sketched in Fig. 2. The barriers for bond rupture without force $\Delta U^{\ddagger} = \Delta H^{\ddagger}(0)$ and with force $\Delta H^{\ddagger}(F)$ are indicated.

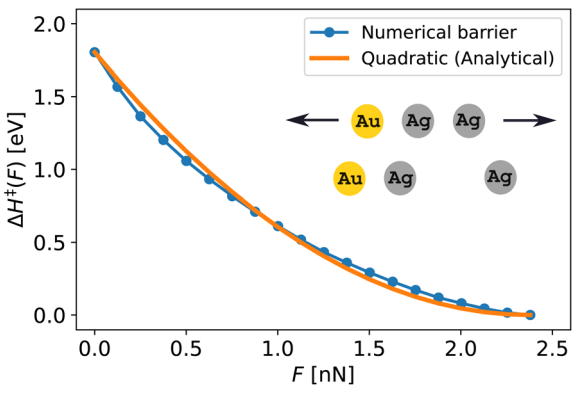

Fig. 2 Barriers for breaking of the Ag–Ag bond under the constraint of a given external force F applied to the outer Au and Ag atoms. The numerical barrier (determined by an explicit inclusion of the external force) is compared to the analytical expression of eqn (2). The setup of the $AuAg_2$ model is sketched.

values completely define the form of the barrier according to eqn (2).

Alternatively, we may also determine the force dependent barrier using the external force is explicitly included (EFEI) strategy,[48,52] where the potential at a fixed external force as in Fig. 1 is analyzed. This strategy leads to a barrier that interpolates between $\Delta H^{\ddagger}(F=0)=\Delta U^{\ddagger}$ and $\Delta H^{\ddagger}(F_{\max})=0$. Its form is closely resembled by the quadratic barrier from eqn (2).

The analytic expression from eqn (2) may therefore be used to derive additional analytic results to predict bond rupture at nonzero temperature. Bond breaking induced by thermal fluctuations is a probabilistic process. Denoting the probability that the bond is intact as P and assuming first order transitions,[41] P follows

$$\frac{\mathrm{d}P}{\mathrm{d}t}=-kP+k_r[1-P], \tag{4}$$

where k is the transition rate for bond breaking (depending on the barrier discussed above) and k_r is the rate for bond reforming.[43] All quantities depend on time t either directly or indirectly which is suppressed for clarity here. We restrict to strong bonds with $\Delta U^{\ddagger}\gg k_{\mathrm{B}}T$ as is typical for chemically bonded species addressed in SMFS experiments. This means that the bond is intact ($P=1$) at $t=0$ when no force is applied. The term involving k_r can be neglected for $1-P\ll P$ (the condition for initial times and strong bonds) or when $k_r\ll k$ as expected for large forces occurring at later times. We will therefore set $k_r=0$ in what follows. A similar approach is taken by Garg,[39] where $P(t)$ is denoted as $W(t)$, and Hummer and Szabo,[40] where $P(t)$ is denoted by $S(t)$. The model by Friddle *et al.*[43] also considers small initial barriers, where bond reforming gets important and k_r can not be neglected.

Further simplifications can be achieved by considering a constant loading rate α[35,39] such that the external force at a given time t satisfies $F=\alpha t$. This assumption differs from that of a constant velocity of the surrounding of the bond sometimes used,[53] but should be similar if the connected cantilever and polymer spring constant k_c is much smaller than the spring constant of the bond k. This is practically always the case for the strong chemical bonds considered here as the spring constant of the environment k_c typically involves thousands of comonomers including the atomic force microscopy cantilever. This results in a very small total effective spring constant k_{total}, for which the loading rate is proportional to velocity v as $\alpha=k_{\mathrm{total}}v$, where $k_{\mathrm{total}}\approx k_c$ (for $k_c\ll k$) is spring constant of system. The constant loading rate then defines the time required to reach the maximal force as $t_{\max}=F_{\max}/\alpha$.

With the force given by $F=\alpha t$ at all times and setting $k_r=0$, we may replace $t=ft_{\max}$ by $f=F/F_{\max}$ and write eqn (4) as[35]

$$\frac{\partial P}{\partial f}=-t_{\max}k(f)P(f)=-\frac{t_{\max}}{\tau}\kappa(f)P(f). \tag{5}$$

Here we have defined the relative rate

$$\kappa(f)=\frac{k(f)}{k(0)}=\exp(\beta[\Delta U^{\ddagger}-\Delta H^{\ddagger}(f)]) \tag{6}$$

with inverse thermal energy $\beta^{-1}=k_{\mathrm{B}}T$, k_{B} denoting the Boltzmann constant and T the absolute temperature. We have expressed the rate without force by the theoretical lifetime of the bond $\tau=1/k\,(f=0)$, despite that this is a theoretical time only, that disregards bond-reforming. Usually $\tau\gg t_{\max}$. ‡.

Eqn (5) can be formally integrated to lead to

$$P(f)=P(f_0)\exp\left(-\frac{t_{\max}}{\tau}\int_{f_0}^{f}\kappa\left(f'\right)\mathrm{d}f'\right), \tag{7}$$

an integral that can be analytically solved for some special $\Delta H^{\ddagger}(f)$. First to third order derivatives of $P(f)$ w.r. to f can be conveniently be expressed in terms of P and κ as given by eqn (S3), (S5) and (S7) in SI.

The distribution $\partial P/\partial f$ determines the most probable relative force f^* measured in the experiment *via*[7,55,56]

$$f^*=\int_0^{\infty}f'\frac{\partial P\left(f'\right)}{\partial f'}\mathrm{d}f'. \tag{8}$$

This function is usually highly peaked,[35,57] such that within the peaking approximation the most probable force f^* will be that at the maximum, *i.e.* f where

$$\partial^2P(f)/\partial f^2=0 \tag{9}$$

(note that $\int_0^{\infty}(\partial P/\partial f)\mathrm{d}f=1$). Eqn (9) can be analytically solved for the Bell barrier from eqn (3), and we get[36,47]

$$f^*=\frac{1}{2\beta\Delta U^{\ddagger}}\log\left(2\beta\Delta U^{\ddagger}\frac{\tau}{t_{\max}}\right). \tag{10}$$

Analytic integration is also possible the quadratic form of the barrier from eqn (2) as detailed in Eqs. (S10–S18) resulting in

$$f^*=1-\sqrt{\frac{1}{2\beta\Delta U^{\ddagger}}W\left(\frac{1}{2\beta\Delta U^{\ddagger}}\frac{{t_{\max}}^2}{\hbar^2\beta^2}\right)}. \tag{11}$$

Here $W(x)$ denotes the Lambert W function. The arguments entering eqn (11) are the ratio of the bond energy by thermal energy (through $2\beta\Delta U^{\ddagger}$) and the time needed to reach $F_{\max}$ relative to the thermal attempt time to break the bond through $t_{\max}/(\hbar\beta)$.

In order to get a feeling about the validity of the peaking approximation, the distributions $\partial P/\partial F{=}F_{\max}^{-1}\partial P/\partial f$ are shown in Fig. 3 for different loading rates and temperatures. We have used the analytic quadratic barrier eqn (2) using $\Delta U^{\ddagger}$ and $F_{\max}$ from $AuAg_2$. Similar distributions appear for the decay in Josephson junctions,[57] where an increasing external flux represents the increasing force as was noted already by Garg.[39] These distributions are peaked in all cases and the peak position is always at forces smaller than $F_{\max}$. Increasing the loading rate (pulling speed) increases the mean force corresponding to the peak as there is less time to overcome the barrier at higher α.

‡ This assumption breaks down for very soft bonds as occurring in biological systems.[54]

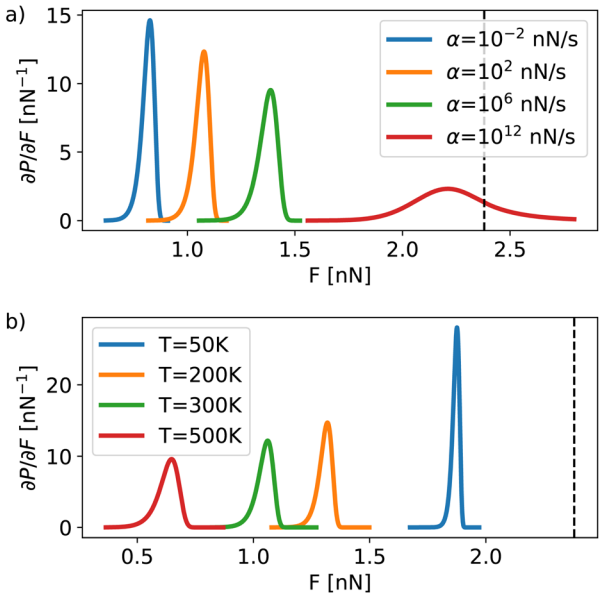

Fig. 3 $\partial P/\partial F$ of the $AuAg_2$ molecule for (a) various loading rates at $T = 300$ K and (b) different temperatures at $\alpha = 100$ nN s^{-1}. The broken line indicates F_{max}.

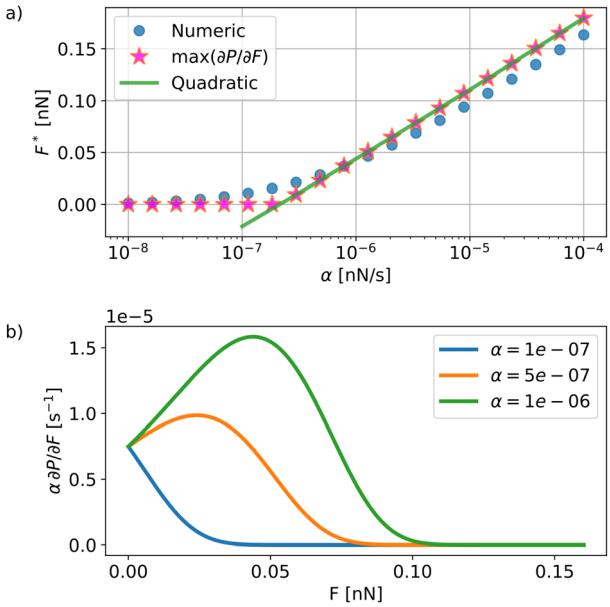

Fig. 4 (a) Most probable force from eqn (8) (Numeric), from eqn (9) (Quadratic), and from max ($\partial P/\partial f$) depending on loading rate at $T = 500$ K. (b) The probability derivative distribution scaled by the loading rate α when the peak position goes towards negative values.

The distribution gets significantly broader with increasing α as the potential flattens with increasing force.

The dependence on temperature is opposite to that on α. Increasing the temperature allows to overcome higher barriers which leads to peak positions at lower force. Increasing T also leads to a broadening of the distribution, such that the distributions get broader for smaller most probable forces in contrast to the effect of increasing α.

It could be estimated from Fig. 3 that the peak position can also appear at negative values of f if α gets very small [*c.f.* Fig. 4a] or if the temperature gets very large. This is indeed the case for

$$\frac{t_{max}}{\tau} > 2\beta\Delta U^{\ddagger} \tag{12}$$

as seen from eqn (10) directly, but can also be proven for eqn (11) (*c.f.* eqn (S20) in SI). This is only the case for extremely small relative forces where the back reaction would play a significant role,[43,45] however.

Fig. 4b depicts the distribution of $\partial P/\partial F$ with decreasing loading rate α values. The distribution is no longer peaked in the positive force direction and thus the estimation of f^* from eqn (9) breaks down as it ultimately leads to negative values. However, the most probable force from eqn (8) is strictly positive even at lower forces.

Fig. 5 shows the most probable force for a large range of loading rates (keeping temperature, $T = 300$ K constant) and temperatures (keeping loading rate, $\alpha = 10$ nN s^{-1} constant). The errorbars for numerical values are determined by the full width at half measurement (FWHM) of the dP/dF distribution. The shaded region indicating the error of the Bell prediction is obtained from eqn (S31). The analytic prediction based on the quadratic barrier closely follows the numeric integration except of the region where negative values appear (for very low forces).

The Bell model is accurate only for low loading rates[40] and high temperatures. Hence it is useful for approximations at low forces only. Additionally, the Bell uncertainty can only describe the increase of the width for large temperatures, but the dependence on the loading rate is not covered as is explicit from eqn (S31). Most probable force and error estimates from the literature[39,42,43,49,58,59] are discussed in detail using a simple example in SI.

Comparison to single molecule force spectroscopy experiments

We have shown above that the dissociation energy $\Delta U^{\ddagger}$ and the maximal force that the bond can withstand F_{max} determine the most probable force measured in the experiment through eqn (11). The similarity of force dependent barriers with the

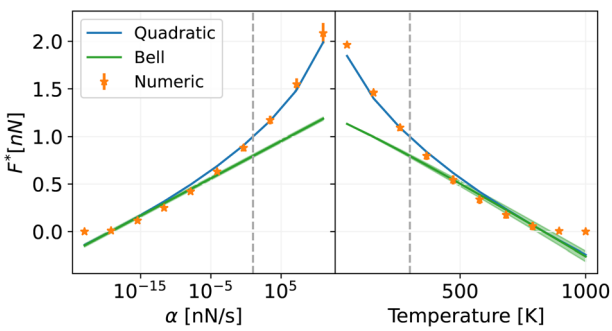

Fig. 5 Most probable force for $AuAg_2$ molecule at various loading rates (left, for $T = 300$ K) and temperatures (right, for $\alpha = 10$ nN s^{-1}). Eqn (8) (Numeric), eqn (10) (Bell) and eqn (11) (Quadratic) are compared.

quadratic form seen in our toy model above and in other cases[8,35,36] suggests that these two quantities are most important and may be sufficient for an accurate estimate of rupture forces measured in SMFS experiments.

We test this assumption for available experimental data from the literature for force opening reactions of cyclopropanes[13,15,16,60,61] and benzocyclobutenes.[6,16] These types of monomers were investigated in the literature within SMFS experiments in many variants and represent non-trivial reactions involving the re-arrangements of multiple bonds. The force induced reactions are illustrated in Fig. 6, where the triangular cyclopropane is re-arranged to form a double and a single bond *via* movement of one of the halogens, while the benzocyclobutenes open the cyclobutene square to form two double bonds when forces are applied. The observed rupture forces are influenced by side groups as well as by variation of the halogens in cyclopropanes. Detailed schematics of all the reactions considered can be found in SI. An extensive investigation of these compounds using COGEF considering step size of 0.075 Å did see some correlations, but was unable to get forces similar to the experimental measurements.[32]

The basic ingredients we need are $\Delta U^{\ddagger}$ and $F_{\max}$, which we calculate within density functional theory (DFT) as implemented in the GPAW package.[62–64] GPAW applies the projector augmented wave (PAW) method,[65] where the smooth wave functions are represented on real space grids with grid spacing of 0.2 Å, while we used grid spacing of 0.1 Å for the smooth electron density. The exchange–correlation functional is approximated as devised by Perdew, Burke and Ernzerhof (PBE).[66]

The question arises about the best method to evaluate $\Delta U^{\ddagger}$ and $F_{\max}$. The first idea may be to use a COGEF calculation[32] *via* the maximal energy and the maximal force observed. While this approach gives good estimates for $F_{\max}$, it generally leads to an overestimation of the dissociation energy. The overestimation is larger for a softer elastic environment coupled to the bond, as soft elastic environments are able to absorb large amounts of energy *via* the applied force.[36] This environment consists of the rest of the monomer-molecule surrounding the bond that breaks as well as co-monomers considered in the calculation. A larger model (which is would appear superior at first sight) therefore worsens the effect. In order to avoid these extra contributions, we determine the barrier in absence of force $\Delta U^{\ddagger} = \Delta H^{\ddagger}(F = 0)$ *via* nudged elastic band calculations.[51,67]

We have considered the medium sized monomers (*i.e.* ring molecule and a two carbon atom chain on either side) for each molecule, as we did not observe major changes by increasing the monomer size further (detailed analysis is given in SI). The stress induced pericyclic ring opening in molecules is suspected to steer the reaction in *a* direction away from thermally induced lower barrier reaction pathway.[68] These thermally activated reactions are in accordance with conservation of orbital symmetry as explained by Woodward–Hoffmann (WH)[69] and Woodward–Hoffmann–DePuy (WHD)[70] rules. It was shown computationally for benzocyclobutenes[22,71] and cyclopropanes[5,26] and also proved experimentally[4–6] that the force induced activation may not always agree with these rules. In cases where forbidden reactions occur in COGEF, the expected product state in accordance with the WH/WHD rules was considered to calculate $\Delta U^{\ddagger}$. This ensures the use of the correct thermal activation barrier (see SI for details).

Using the monomer properties $\Delta U^{\ddagger}$ and $F_{\max}$, the missing ingredients to predict the most probable rupture force F^* are the loading rate and the temperature at which the SMFS experiment is performed. Room temperature was assumed throughout. The experimental loading rate specified in the references is directly chosen.[13] In cases where the values are not specified, we estimate it using the product of spring constant and experimental velocity (as $\alpha = k_{\text{total}} v$). The total spring constant of the experimental setup k_{total} is obtained from a linear fit of the experimental SMFS force *vs.* elongation. If this calculated value results in a value larger than the given cantilever spring constant, we consider the latter for the calculation of loading rate (see Tabs. S1 and S3 in SI for details).

Using these values, we compare our predictions using eqn (11) to the measured rupture forces[4,6,13–16] in Fig. 7. The horizontal error bars correspond to the experimental error range and the vertical error bars correspond to the prediction errors (Eq. (S67) in SI), which is close to the width of the probability density distribution. We obtain very good agreement between our model and the experiment over a large force range. The prediction is quantitative and much better than the usage of

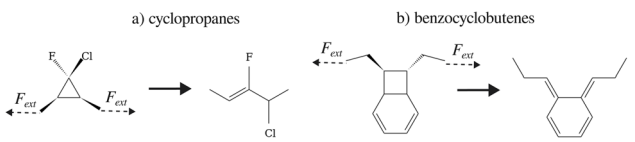

Fig. 6 General reaction schemes for (a) cyclopropanes and (b) benzocyclobutenes.

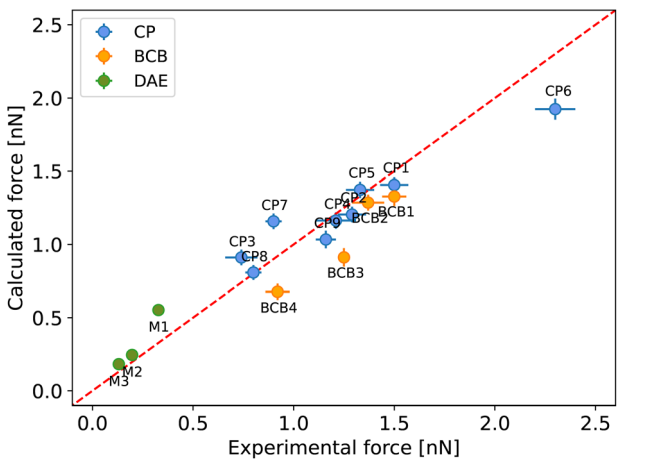

Fig. 7 Comparison our predicted most probable force to experimental results for cyclopropanes (CP), benzocyclobutenes (BCB) and diarylethenes (DAE). The schematics of reactions, experimental and calculated values for the molecules can be found in SI (Table S3). The meaning of the errorbars is explained in the text. The broken line indicates perfect agreement.

F_{max}[32] as seen explicitly in Fig. S9 of SI. Our description is thus able to predict experimentally observed rupture forces directly from this minimal set of parameters, where only $\Delta U^{\ddagger}$ and F_{max} obtained from DFT enter.

We have also incorporated diarylethene (DAE) mechanophores that were investigated in a recent study[72] into the estimation of the most probable forces from our model. The DAEs were reported to undergo mechanically driven noncovalent transformations showing pronounced lever arm effects. We have used the COGEF F_{max} and the thermal barriers $\Delta U^{\ddagger}$ for rotation for these molecules as given in this study. The loading rate is estimated (0.9 nN s^{-1} for a velocity of 3000 Å s^{-1}) using the cantilever spring constant from the force–extension curve similar to other molecules discussed in SI. Inclusion of these additional molecules expands the diversity as comparably low forces were detected (Fig. 7). We also get very good agreement in our prediction of the most probable force with the measured one for this noncovalent, but still barrier-controlled force-induced transition.

Conclusions

In conclusion, we have derived a closed form for the prediction of most probable bond-rupture forces as measured in single molecule force spectroscopy experiments. The nature of the bond exposed to external forces can be conveniently described by two key parameters which are the bond energy in absence of force and the maximal force that the bond can withstand. These two quantities are usually sufficient to characterize the force-dependent barrier until a bond breaks to good accuracy. The approximative quadratic form assumed naturally leads to the famous Bell model for small forces. These necessary properties of the bond can be obtained *via* density functional theory calculations using force-free transition state modeling and a COGEF calculation.

Assuming a constant force increase, the rest is statistics as the bond is broken by thermal fluctuations. The experimentally observed most probable breaking force is governed by the time scales of the force increase and the attempt frequency to break the bond. This leads to a closed and simple form for the prediction of the forces measured in experiment in eqn (11) without the involvement of any empirical parameter.

The effectiveness and accuracy of this description is tested on rupture forces from ring opening reactions of cyclopropanes and benzocyclobutenes as well as for diarylethene noncovalent rearrangements reported in the literature. We find very good agreement of our predicted forces and the experimentally observed ones in all cases with a coefficient of determination of $R^2 = 90.1\%$.

We expect that the approximations adopted are widely applicable also to other types of bond openings or bond formations under external stimuli. A similar description may also be valid for pressure or shear induced reactions, where the external force is replaced by external pressure p, or more generally the stress tensor σ. Usually, a linear approximation defining an activation volume $V^{\ddagger}$[73] similar to the Bell length $x^{\ddagger}$ is applied, but also descriptions going beyond that exist.[74] Very similar expressions as eqn (11) for the most probable pressure should appear under a constant pressure increase defining the loading rate and it is an interesting question whether $V^{\ddagger}$ can also be related to $\Delta U^{\ddagger}$ at $p = 0$ and the maximal p_{max} where the reaction occurs without barrier. This may help us understand the puzzling large variation of activation volumes observed.[75] The general form of the deformation tensor σ will require modifications and the approximation may also break down for very complicated barriers that can not be described by the simple quadratic form of $\Delta H^{\ddagger}(F)$, like retro-Diels–Alder bond openings, however.[8]

Conflicts of interest

There are no conflicts of interest to declare.

Data availability

The software used is open source and can be installed cross platform using pip (for Python): the atomic simulation environment ASE (https://www.ase-lib.org/ase/atoms.html), GPAW (https://www.gpaw.readthedocs.io) and cogef (https://www.cogef.gitlab.io/cogef/index.html). The relaxed structures of the molecules, their force free transition states and COGEF trajectories will be openly published in a gitlab repository (https://www.gitlab.com/ag_walter).

Supplementary information (SI) is available. See DOI: https://doi.org/10.1039/d5mr00129c.

Acknowledgements

M. W. thanks L. Mayrhofer for discussions about activation volumes. The authors are grateful for funding by the Deutsche Forschungsgemeinschaft (DFG, German Research Foundation) under Germany's Excellence Strategy-EXC-2193/1-390951807 and WA 1687/11-1. The authors acknowledge computational resources by the state of Baden-Württemberg through bwHPC and the German Research Foundation (DFG) through grant no INST 39/963-1 FUGG (bwForCluster NEMO) and INST 40/575-1 FUGG (bwForCluster JUSTUS2).

References

1 L. Yang, Z. Chen, C. A. Goult, T. Schlatzer, R. S. Paton and V. Gouverneur, *Nature*, 2025, 1–7.
2 J.-L. Do and T. Friščić, *ACS Cent. Sci.*, 2017, **3**, 13.
3 T.-G. Hsu, S. Liu, X. Guan, S. Yoon, J. Zhou, W.-Y. Chen, S. Gaire, J. Seylar, H. Chen, Z. Wang, J. Rivera, L. Wu, C. J. Ziegler, R. McKenzie and J. Wang, *Nat. Commun.*, 2023, **14**, 225.
4 J. Wang, T. B. Kouznetsova, Z. S. Kean, L. Fan, B. D. Mar, T. J. Martínez and S. L. Craig, *J. Am. Chem. Soc.*, 2014, **136**, 15162.
5 J. M. Lenhardt, M. T. Ong, R. Choe, C. R. Evenhuis, T. J. Martinez and S. L. Craig, *Science*, 2010, **329**, 1057.
6 J. Wang, T. B. Kouznetsova, Z. Niu, A. L. Rheingold and S. L. Craig, *J. Org. Chem.*, 2015, **80**, 11895.

7 F. Kempe, O. Brügner, H. Buchheit, S. N. Momm, F. Riehle, S. Hameury, M. Walter and M. Sommer, *Angew. Chem., Int. Ed.*, 2018, **57**, 997.
8 M. Walter, D. Linsler, T. König, C. Gäbert, S. Reinicke, M. Moseler and L. Mayrhofer, *J. Phys. Chem. Lett.*, 2023, **14**, 1445.
9 R. Hertel, M. Raisch, M. Walter, G. Reiter and M. Sommer, *Angew. Chem., Int. Ed.*, 2024, e202409369.
10 H. Traeger, D. Kiebala, C. Calvino, Y. Sagara, S. Schrettl, C. Weder and J. M. Clough, *Mater. Horiz.*, 2023, **10**, 3467.
11 M. Raisch, G. Reiter and M. Sommer, *ACS Macro Lett.*, 2022, **11**, 760.
12 M. Grandbois, M. Beyer, M. Rief, H. Clausen-Schaumann and H. E. Gaub, *Science*, 1999, **283**, 1727.
13 H. M. Klukovich, T. B. Kouznetsova, Z. S. Kean, J. M. Lenhardt and S. L. Craig, *Nat. Chem.*, 2013, **5**, 110.
14 O. N. Faza, C. S. López, R. Álvarez and A. R. de Lera, *J. Org. Chem.*, 2004, **69**, 9002.
15 J. Wang, T. B. Kouznetsova, Z. S. Kean, L. Fan, B. D. Mar, T. J. Martínez and S. L. Craig, *J. Am. Chem. Soc.*, 2014, **136**, 15162.
16 J. Wang, T. B. Kouznetsova, Z. Niu, M. T. Ong, H. M. Klukovich, A. L. Rheingold, T. J. Martinez and S. L. Craig, *Nat. Chem.*, 2015, **7**, 323.
17 W. Cai, J. T. Bullerjahn, M. Lallemang, K. Kroy, B. N. Balzer and T. Hugel, *Chem. Sci.*, 2022, **13**, 5734.
18 S. Akbulatov, Y. Tian and R. Boulatov, *J. Am. Chem. Soc.*, 2012, **134**, 7620.
19 S. W. Schmidt, M. K. Beyer and H. Clausen-Schaumann, *J. Am. Chem. Soc.*, 2008, **130**, 3664.
20 S. W. Schmidt, A. Kersch, M. K. Beyer and H. Clausen-Schaumann, *Phys. Chem. Chem. Phys.*, 2011, **13**, 5994.
21 S. W. Schmidt, M. F. Pill, A. Kersch, H. Clausen-Schaumann and M. K. Beyer, *Faraday Discuss.*, 2014, **170**, 357.
22 M. T. Ong, J. Leiding, H. Tao, A. M. Virshup and T. J. Martínez, *J. Am. Chem. Soc.*, 2009, **131**, 6377.
23 P. Dopieralski, P. Anjukandi, M. Rückert, M. Shiga, J. Ribas-Arino and D. Marx, *J. Mater. Chem.*, 2011, **21**, 8309.
24 P. Dopieralski, J. Ribas-Arino and D. Marx, *Angew. Chem., Int. Ed.*, 2011, **50**, 7105.
25 M. Wollenhaupt, M. Krupička and D. Marx, *ChemPhysChem*, 2015, **16**, 1593.
26 M. Wollenhaupt, C. Schran, M. Krupička and D. Marx, *ChemPhysChem*, 2018, **19**, 837.
27 J. Wang, T. B. Kouznetsova, R. Boulatov and S. L. Craig, *Nat. Commun.*, 2016, **7**, 1.
28 M. K. Beyer, *J. Chem. Phys.*, 2000, **112**, 7307.
29 J. Ribas-Arino and D. Marx, *Chem. Rev.*, 2012, **112**, 5412.
30 J. R. Hemmer, C. Rader, B. D. Wilts, C. Weder and J. A. Berrocal, *J. Am. Chem. Soc.*, 2021, **143**, 18859.
31 J. R. Hemmer, V. Bauernfeind, C. Rader, M. Petroselli, C. Weder and J. A. Berrocal, *Macromolecules*, 2023, **56**, 8614.
32 I. M. Klein, C. C. Husic, D. P. Kovács, N. J. Choquette and M. J. Robb, *J. Am. Chem. Soc.*, 2020, **142**, 16364.
33 C. R. Wick, E. Topraksal, D. M. Smith and A.-S. Smith, *Forces Mech.*, 2022, **9**, 100143.
34 I. V. Pobelov, K. P. Lauritzen, K. Yoshida, A. Jensen, G. Meszaros, K. W. Jacobsen, M. Strange, T. Wandlowski and G. C. Solomon, *Nat. Commun.*, 2017, **8**, 1.
35 F. Hanke and H. J. Kreuzer, *Phys. Rev. E:Stat., Nonlinear, Soft Matter Phys.*, 2006, **74**, 1.
36 S. Khodayeki, W. Maftuhin and M. Walter, *ChemPhysChem*, 2022, e202200237.
37 Y. Sun, I. Kevlishvili, T. B. Kouznetsova, Z. P. Burke, S. L. Craig, H. J. Kulik and J. S. Moore, *Chem*, 2024, **10**, 3055.
38 Y. Sun, F. Xie and J. S. Moore, *J. Am. Chem. Soc.*, 2024, **146**, 31702.
39 A. Garg, *Phys. Rev. B*, 1995, **51**, 15592.
40 G. Hummer and A. Szabo, *Biophys. J.*, 2003, **85**, 1.
41 O. K. Dudko, G. Hummer and A. Szabo, *Phys. Rev. Lett.*, 2006, **96**, 108101.
42 J. T. Bullerjahn, S. Sturm and K. Kroy, *Nat. Commun.*, 2014, **5**, 4463.
43 R. W. Friddle, A. Noy and J. J. De Yoreo, *Proc. Natl. Acad. Sci. U.S.A.*, 2012, **109**, 13573.
44 W. Cai, M. Jäger, J. T. Bullerjahn, T. Hugel, S. Wolf and B. N. Balzer, *Nano Lett.*, 2023, **23**, 4111.
45 J. T. Bullerjahn and G. Hummer, *Phys. Rev. Res.*, 2022, **4**, 033097.
46 W. Kauzman and H. Eyring, *J. Am. Chem. Soc.*, 1940, **62**, 3113.
47 E. Evans and K. Ritchie, *Biophys. J.*, 1997, **72**, 1541.
48 T. Stauch and A. Dreuw, *Chem. Rev.*, 2016, **116**, 14137.
49 G. I. Bell, *Science*, 1978, **200**, 618.
50 S. M. Avdoshenko and D. E. Makarov, *J. Chem. Phys.*, 2015, **142**, 174106.
51 A. H. Larsen, J. J. Mortensen, J. Blomqvist, I. E. Castelli, R. Christensen, M. Dułak, J. Friis, M. N. Groves, B. Hammer, C. Hargus, E. D. Hermes, P. C. Jennings, P. B. Jensen, J. Kermode, J. R. Kitchin, E. L. Kolsbjerg, J. Kubal, K. Kaasbjerg, S. Lysgaard, J. B. Maronsson, T. Maxson, T. Olsen, L. Pastewka, A. Peterson, C. Rostgaard, J. Schiøtz, O. Schütt, M. Strange, K. S. Thygesen, T. Vegge, L. Vilhelmsen, M. Walter, Z. Zeng and K. W. Jacobsen, *J. Phys.: Condens. Matter*, 2017, **29**, 273002.
52 J. Ribas-Arino, M. Shiga and D. Marx, *Angew. Chem., Int. Ed.*, 2009, **48**, 4190.
53 O. K. Dudko, A. E. Filippov, J. Klafter and M. Urbakh, *Proc. Natl. Acad. Sci. U. S. A.*, 2003, **100**, 11378.
54 F. Rico, A. Russek, L. González, H. Grubmüller and S. Scheuring, *Proc. Natl. Acad. Sci. U. S. A.*, 2019, **116**, 6594.
55 P. M. Williams, *Anal. Chim. Acta*, 2003, **479**, 107.
56 O. Brügner and M. Walter, *Phys. Rev. Mater.*, 2018, **2**, 1.
57 J. Kurkijärvi, *Phys. Rev. B*, 1972, **6**, 832.
58 O. K. Dudko, J. Mathé, A. Szabo, A. Meller and G. Hummer, *Biophys. J.*, 2007, **92**, 4188.
59 R. W. Friddle, *Phys. Rev. Lett.*, 2008, **100**, 138302.
60 J. Wang, T. B. Kouznetsova and S. L. Craig, *J. Am. Chem. Soc.*, 2014, **137**, 11554.
61 D. Wu, J. M. Lenhardt, A. L. Black, B. B. Akhremitchev and S. L. Craig, *J. Am. Chem. Soc.*, 2010, **132**, 15936.
62 J. J. Mortensen, L. B. Hansen and K. W. Jacobsen, *Phys. Rev. B*, 2005, **71**, 035109.

63 J. Enkovaara, C. Rostgaard, J. J. Mortensen, J. Chen, M. Dułak, L. Ferrighi, J. Gavnholt, C. Glinsvad, V. Haikola, H. A. Hansen, H. H. Kristoffersen, M. Kuisma, A. H. Larsen, L. Lehtovaara, M. Ljungberg, O. Lopez-Acevedo, P. G. Moses, J. Ojanen, T. Olsen, V. Petzold, N. A. Romero, J. Stausholm-Møller, M. Strange, G. A. Tritsaris, M. Vanin, M. Walter, B. Hammer, H. Häkkinen, G. K. H. Madsen, R. M. Nieminen, J. K. Nørskov, M. Puska, T. T. Rantala, J. Schiøtz, K. S. Thygesen and K. W. Jacobsen, *J. Phys. Condens. Matter.*, 2010, **22**, 253202.

64 J. J. Mortensen, A. H. Larsen, M. Kuisma, A. V. Ivanov, A. Taghizadeh, A. Peterson, A. Haldar, A. O. Dohn, C. SchÄfer, E. Ö. Jonsson, E. D. Hermes, F. A. Nilsson, G. Kastlunger, G. Levi, H. Jonsson, H. Häkkinen, J. Fojt, J. Kangsabanik, J. Sødequist, J. Lehtomäki, J. Heske, J. Enkovaara, K. T. Winther, M. Dulak, M. M. Melander, M. Ovesen, M. Louhivuori, M. Walter, M. Gjerding, O. Lopez-Acevedo, P. Erhart, R. Warmbier, R. Würdemann, S. Kaappa, S. Latini, T. M. Boland, T. Bligaard, T. Skovhus, T. Susi, T. Maxson, T. Rossi, X. Chen, Y. L. A. Schmerwitz, J. Schiøtz, T. Olsen, K. W. Jacobsen and K. S. Thygesen, *J. Chem. Phys.*, 2024, **160**, 092503.

65 P. E. Blöchl, *Phys. Rev. B*, 1994, **50**, 17953.

66 J. P. Perdew, K. Burke and M. Ernzerhof, *Phys. Rev. Lett.*, 1996, **77**, 3865.

67 G. Henkelman, G. Jóhannesson and H. Jónsson, in Methods for Finding Saddle Points and Minimum Energy Paths, ed. S. D. Schwartz, *Theoretical Methods in Condensed Phase Chemistry, Progress in Theoretical Chemistry and Physics*, Springer Netherlands, Dordrecht 2002, pp. 269–302.

68 R. B. Woodward and R. Hoffmann, *Angew Chem. Int. Ed. Engl.*, 1969, **8**, 781.

69 R. B. Woodward and R. Hoffmann, *J. Am. Chem. Soc.*, 1965, **87**, 395.

70 C. H. DePuy, *Acc. Chem. Res.*, 1968, 33–41.

71 C. R. Hickenboth, J. S. Moore, S. R. White, N. R. Sottos, J. Baudry and S. R. Wilson, *Nature*, 2007, **446**, 423.

72 C. Zhang, T. B. Kouznetsova, B. Zhu, L. Sweeney, M. Lancer, I. Gitsov, S. L. Craig and X. Hu, *J. Am. Chem. Soc.*, 2025, **147**, 2502.

73 A. Martini and S. H. Kim, *Tribol. Lett.*, 2021, **69**, 150.

74 N. Hopper, F. Sidoroff, J. Cayer-Barrioz, D. Mazuyer, B. Chen and W. T. Tysoe, *RSC Mechanochem.*, 2024, **1**, 402.

75 Z. Li and I. Szlufarska, *Phys. Rev. Lett.*, 2021, **126**, 076001.

